RSC Advances

ROYAL SOCIETY OF CHEMISTRY

www.rsc.org/advances

Journal Name

RSCPublishing

ARTICLE

Dual channel selective fluorescent detection of Al^{3+} and PPi in mixed aqueous media: DFT studies and cell imaging applications.

Cite this: DOI: 10.1039/x0xx00000x

Received 00th January 2015,
Accepted 00th January 2015

DOI: 10.1039/x0xx00000x

www.rsc.org/

Rabiul Alam[a], Tarun Mistri[a], Rahul Bhowmick[a], Atul Katarkar[b], Keya Chaudhuri[b] and Mahammad Ali[a]*

Abstract

A new, easily synthesizable chemosensor, **DFC-EN-*p*-Ph-NO_2,** derived by the Schiff base condensation between 2,6-diformyl-*p*-cresol and N-(4-nitrophenyl)ethylenediamie, with potential N_4O donor atoms was found to act as a double channels (colori- and fluorimetric) dual sensors towards Al^{3+} and PPi emitting at 486 nm (blue region) and 534 nm (green region), respectively in MeOH-H_2O (8:2, v/v) at pH 7.2 (10 mM HEPES buffer), μ = 0.05 M (LiCl), temperature 25 ºC. The binding stoichiometries and formation constants of the sensor towards both Al^{3+} and PPi were determined by the combined UV-Vis and fluorescence titrations and Job's method, and confirmed by MS (m/z) studies. The corresponding detection limits as calculated by 3σ method are: 7.55 μM and 3.34 μM. The most interesting part of this study is that on addition of 230 μM PPi to an ensemble of **DFC-EN-*p*-Ph-NO_2**–Al^{3+} (20 μM Ligand and 380 μM Al^{3+}) the fluorescence is totally quenched but on further addition of PPi a new emission peak appears at 534 nm. All biologically relevant metal ions and toxic heavy metals did not interfere with the detection of Al^{3+} ion. Owing to its bio-compatibility with respect to its good solubility in mixed organo-aqueous media (MeOH/H_2O) and cell permeability with no or negligible cytotoxicity provide good opportunity towards *in-vitro* cell imaging studies of these ions. In particular, the fluorescent detection of PPi was not interfered by the presence of 400 μM of ATP or Pi although the most reported PPi sensors that work in aqueous solution displayed cross-sensitivities toward ATP or Pi The obvious excellent sensing capability of **DFC-EN-*p*-Ph-NO_2** towards PPi and Al^{3+} were further scrutinized in HCT116 cell lines without much cytotoxicity. The modes of 1:1 binding of **DFC-EN-*p*-Ph-NO_2** towards Al^{3+} and PPi were delineated by DFT calculations.

Journal Name RSCPublishing

ARTICLE

Introduction

Pyrophosphate ($P_2O_7^{4-}$, PPi), a hydrolysis product of ATP and other nucleotide triphosphates, is involved in various anabolic and bioenergetics processes.[1-3] Several cell signalling processes utilize adenylatecyclase (guanylatecyclase) that catalyze the conversion of ATP (GTP) to cAMP (cGMP) and PPi.[4,5] PPi is also used as an additive in food (E450), toothpaste, baking powder, and detergents.[6] Thus, the selective detection of PPi is important for monitoring the biological processes mediated by hydrolysis of nucleotide triphosphate to release PPi.

Since the first report on PPi fluorescent sensor by Czarnik[7] this becomes an interesting field of research by chemists and biochemists.[8-11] Most often, these sensors contain metal complexes as the recognition units of phosphates. Zn(II) complexes are frequently used in this context,[12] but other metal ions such as Cu(II),[13] Cd(II),[14] Mn(II),[15] Eu(III),[16] and Tb(III)[17] have been employed as well, however Al^{3+} bound PPi sensor is rare.[18] Even though various types of chemosensors that recognize PPi in water have been reported,[11,19-23] only a few of them had sufficient selectivity for PPi over ATP or Pi in aqueous solutions.

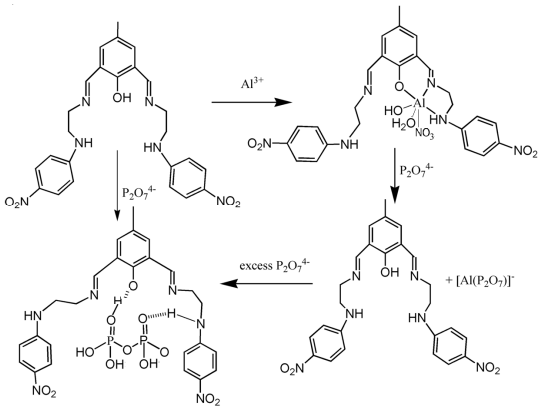

Scheme 1

In **Scheme 1** we describe a turn-on Al^{3+} sensor which can also functions as PPi sensor both in presence and absence of Al^{3+}. The most important aspects of this sensor are that it senses Al^{3+} selectively by fluorescence emission in blue region while PPi sensing occurs in the green region.

Materials and Methods

The starting materials such as *p*-chloro nitrobenzene (Sigma Aldrich), ethylenediamine, diformyl-*p*-cresol (prepared in this laboratory) were used for the preparation of ligands. $Al(NO_3)_3.9H_2O$ was used to prepare Al^{3+}-complex. Solvents like ethanol, diethyl ether and methanol (Merck, India) were of reagent grade and dried before use.

Physical measurements

Elemental analyses were carried out using a Perkin–Elmer 240 elemental analyzer. Infrared spectra (400–4000 cm^{-1}) were recorded in liquid state on a Nickolet Magna IR 750 series-II FTIR spectrometer. ^{1}H-NMR spectra were recorded in DMSO-d_6 on a Bruker 300 MHz NMR spectrometer using tetramethylsilane (δ = 0) as an internal standard. ESI-MS^+ (m/z) of the ligand and Al^{3+}-complex were recorded on a Waters' HRMS spectrometer (Model: XEVO G2QTof). UV-Vis spectra were recorded on an Agilent diode-array spectrophotometer (Model, Agilent 8453). Steady-state fluorescence measurements were performed with a PTI QM-40 spectrofluorometer.

Solution Preparation for UV-Vis Absorption and fluorescence studies

For both UV-Vis and fuorescence titrations, stock solution of 1.0 x 10^{-3} M of the probe **DFC-EN-*p*-Ph-NO_2** was prepared in MeOH. Similarly, another 1.0 x 10^{-3} M stock solution of $Al(NO_3)_3.9H_2O$ and other metal ions were prepared in MeOH-H_2O (8:2, v/v). A solution of MeOH-H_2O (8:2, v/v) containing 10.0 mM HEPES buffer was prepared and pH was adjusted to 7.20 by using HCl and NaOH. Ionic strength was maintained at 20 mM (NaCl) throughout the measurements. 2.5 ml of this buffered solution was pipetted out into a cuvette to which was added 20 μM of the probe and metal ions were added incrementally starting from 0 to 380 μM in a regular interval of volume and UV-Vis and fluorescence spectra were recorded for each solution.

Preparation of N-(2-aminoethyl)-4-nitrobenzenamine (1).

N-(2-aminoethyl)-4-nitrobenzenaminehas been prepared using literature procedure.[24]

Preparation of DFC-EN-*p*-Ph-NO_2 (2).

2,6-Diformyl-*p*-cresol (DFC) was prepared by following a literature procedure.[25] 2,6-Diformyl-*p*cresol(DFC) (1.64 g, 10 mmol) was dissolved in 25 ml EtOH under nitrogen atmosphere. To this solution, N-(2-aminoethyl)-4-nitrobenzenamine (1) (1.81 g, 10 mmol) was added and stirred at room temperature for 2 h, whereupon solid precipitate formed was filtered and washed with diethyl ether and air dried **(Scheme 2)**. It was recrystallized from ethanol to get pure product. Yield, 80%.CHN Analysis for $C_{25}H_{26}N_6O_5$: Calculated (%): C, 61.22; H, 5.34; N, 17.13. Found (%): C, 61.21; H, 5.33; N, 17.14. .^{1}H-NMR (in DMSO-d_6) (δ, ppm): 7.36 (s,2H (NH), 14.04 (s,1H), 2.23 (s, 3-H), 7.48 (s, 2-H), 8.57 (s, 2-H) , 7.98 (d, *J= 9.2*, 4-H), 6.70 (d, *J=9.2*,4H), 3.78 (d, *J=5.0*,4H), 3.50 (d, *J= 5.6*, 4-H) (please see

Fig. S1 for ^{1}H-NMR). ^{13}C-NMR: (300 MHz, DMSO-d_6) δ_{ppm}: 20.27, 43.59, 58.68, 111.42, 121.30, 126.64, 127.02, 132.87, 136.21, 155.01, 159.70, 162.48 (**Fig. S2**).ESI-MS$^+$ (m/z): 491.20(**DFC-EN-*p*-Ph-NO$_2$** + H$^+$) **[Fig. S3]**. IR spectrum (in MeOH): -OH (3499 cm^{-1}),-C=N (1639 cm^{-1}), -NH (3177 Cm^{-1}). (**Fig.S4**)

Synthesis of [Al(DFC-EN-*p*-Ph-NO$_2$-H$^+$)(H$_2$O)(OH)(NO$_3$)]Complex (3).

$Al(NO_3)_2.9H_2O$ (0.375 g, 1 mmol) was dissolved in 10 ml methanol.To this solution, **DFC-EN-*p*-Ph-NO$_2$** (0.350 g, 1.0 mmol.) in 3 mL MeOH was added. The colour of the solution changed to faint yellow. The resulting mixture was stirred for 3 h at room temperature. The volume of the solution was reduced to 5 ml under reduced pressure and diethyl ether (10 mL) was added and kept at 0 °C for 12 h to afford complex **3** as microcrystals. Yield: 0.356 g (~52%). CHN analyses for [**Al(DFC-EN-*p*-Ph-NO$_2$)**$(H_2O)(OH)](NO_3)$] $C_{25}H_{28}N_7O_{10}Al$ (M.W.613.51), Calcd (%): C, 48.94; H,4.60; N, 15.98. Found (%): C, 48.90; H 4.66; N, 15.97. UV-vis. (MeOH): λ_{max} 370 nm (**Fig. 1**).

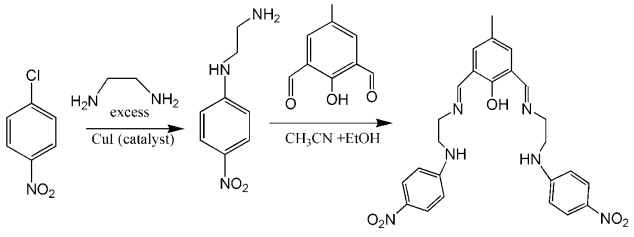

Scheme 2

Cell culture

Human colon cancer (HCT116) cell line, were grown in DMEM supplemented with 10% FBS and antibiotics (penicillin-100 µg/ml; streptomycin-50 µg/ml). Cells were cultured at 37ºC in 95% air, 5% CO_2 incubator.

Cell Cytotoxicity Assay

To determine % cell viability of **DFC-EN-*p*-Ph-NO$_2$**, MTT assay was performed.[26] HCT116 cells (1×10^5 cells/well) were cultured in a 96-well plate at 37°C, and exposed to varying concentrations of 1, 10, 20, 40, 60, 80 and 100 µM of **DFC-EN-*p*-Ph-NO$_2$** for 12 h. 20 µl of MTT solution [5 mg/ml 1X phosphate-buffered saline (PBS)] was added to each well of a 96-well culture plate and again incubated continuously at 37^{0}C for a period of 4 h. All media were removed from wells and 150 µl of DMSO was added to each well and absorbance was measured at 550 nm (EMax Precision MicroPlate Reader, Molecular Devices, USA). All experiments were performed in triplicate and the relative cell viability (%) was expressed as a percentage relative to the untreated control cells.

Cell Imaging Study

HCT116 Cells were cultured and incubated in 35 x10 mm culture dish over coverslip and allowed to incubate with 10µm **DFC-EN-*p*-Ph-NO$_2$** (prepared by dissolving in a mixed solvent (DMSO: water = 1:9 (v/v) in the culture medium) for 30 min at 37 °C. After incubation, cells were washed thrice with 1X PBS; cover slip containing HCT116 cells were allowed to treated with 0µM, 4µM, 6µM, 8µM and 10µM of Al3+ (Experimental Set-I), 0µM, 4µM, 6µM, 8µM and 10µM of PPi (Experimental Set-II) and 0µM, 4µM, 6µM, 8µM and 10µM of Al^{3+}+PPi (Experimental Set-III), incubated for 30 min at 37ºC, washed twice with1X PBS and coverslip were mounted over the slide. Bright field and fluorescence images of HCT116 cells were taken by a fluorescence microscope (Leica DM3000, Germany) with an objective lens of 40X magnification. HCT116 cells showed excellent green fluorescence when **DFC-EN-*p*-Ph-NO$_2$** formed intracellular complex with PPi and blue fluorescence with Al^{3+}.

Results and Discussion

Synthesis and Characterization of DFC-EN-*p*-Ph-NO$_2$

DFC-EN-*p*-Ph-NO_2 was prepared according to the synthetic routes shown in Scheme 2 in 80 % yields.

To an ethanolic solution of 2,6-Diformyl-*p*cresol (DFC) under nitrogen atmosphere was added N-(2-aminoethyl)-4-nitrobenzenamine (**1**) and stirred at room temperature for 2h, whereupon solid precipitate formed was filtered, recrystallized from ethanol to get the pure product. The probe was characterized by various spectroscopic (IR, ^{1}H and ^{13}C NMR) and HRMS analyses. It was further reacted with $Al(NO_3)_2.9H_2O$ to afford complex **3** as microcrystals in 52% yield and characterized analogously. Several attempts to get single crystals for X-ray diffraction studies were failed.

UV-Vis Absorption Studies

The electronic absorption properties of **DFC-EN-*p*-Ph-NO$_2$** (2) were investigated in MeOH:H_20 (8:2, v/v) at pH 7.2 in 10 mM HEPES buffer at µ = 0.05 M (LiCl). The absorption spectrum of the free ligand consists of three absorption bands at 455, 388 and 276 nm which are assigned as π–π*, n–π* and σ–π* transitions, respectively.[27] On gradual addition of Al^{3+} the absorbance of compound **3** at 448 and 270 nm gradually decrease, while, the band at 388 nm gradually shifted to 370 nm producing three well defined isosbestic points at 375, 300 and 250 nm which clearly indicate the transformation of free ligand to its metal-bound state.

$$y = (a+b*c*x^n)/(1+c*x^n) \quad (1)$$

When we plot absorbance as a function of [Al^{3+}] a non-linear curve of decreasing slope was obtained which can be easily solved by using eqn (1),[28] where *a* and *b* are the absorbances in the absence and presence of excess metal ions, respectively, *c* (= K) is the formation constant and *n* is the stoichiometry of the reactions. The non-linear least-squares curve-fit of the absorption titration data (**Fig.1 b**) as a function of [Al^{3+}] gives: $c = K = (2.26 \pm 1.00) \times 10^4$ M^{-1}, $n = 0.93 \pm 0.04$. The 1:1 mole ratio for L-M binding was further determined by JOB's method (**Fig.S5**) and ESI-MS$^+$(m/z)(**Fig. S3a)** studies.

As the reaction between the probe and Al^{3+} was found to be slow we tried to evaluate the rate constants for this reaction under pseudo-first order conditions taking the probe as a minor component [**DFC-EN-*p*-Ph-NO$_2$**] = 20 μM and [Al^{3+}] in large excess (20-200 μM). In each concentration of Al^{3+} the pseudo-first-order rate constants were evaluated by fitting the kinetic traces to a first-order computer-fit program associated with the spectrophotometer. A plot of k_{obs} vs. [Al^{3+}] yields a non-linear curve of decreasing slope. Such dependence could be best described by the following reaction sequence (eqn 2).

$$L + Al^{3+} \underset{}{\overset{Q}{\rightleftharpoons}} L\cdots Al^{3+} \xrightarrow{k} L{-}Al^{3+} \qquad (2)$$

The corresponding rate law could be derived as eqn (3)

$$k_{obs} = \frac{kQ[Al^{3+}]}{1+Q[Al^{3+}]} \qquad (3)$$

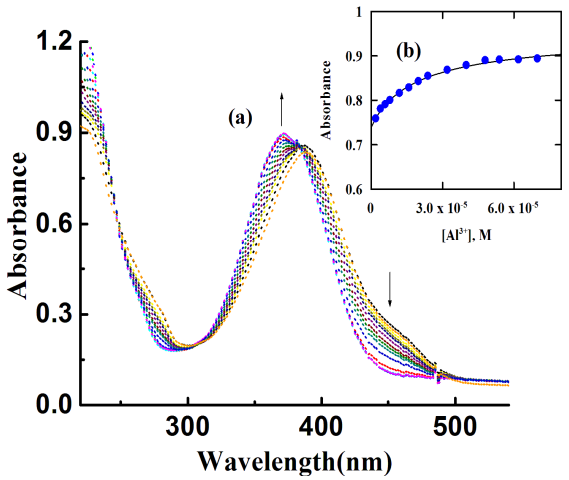

Fig. 1. (a) Absorption titration of with Al^{3+} in MeOH-H_2O (8:2, v/v) in HEPES buffer (10 mM) at pH 7.2; (b) Non- linear curve fitting.

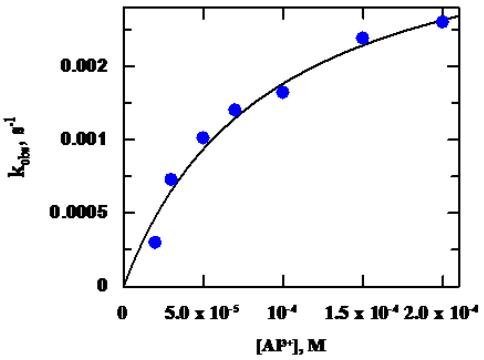

Fig. 2. Non-linear curve-fitting of a plot of k_{obs} vs. [Al^{3+}] for the complexation of Al^{3+} with **DFC-EN-*p*-Ph-NO$_2$** in MeOH-H_2O (8:2, v/v) at pH 7.2 (10 mM HEPES buffer), μ = 0.05 M (LiCl), temperature 25ºC

Non-linear least-squares fitting of k_{obs} as a function of [Al^{3+}] gives k = (2.6 ± 0.30) x 10^{-3} $M^{-1}s^{-1}$ and Q = (1.10 ± 0.23) x 10^4 M^{-1}. Here Q signifies the initial inner-sphere association between the probe and the metal ion. **Figure 3** displays a time resolved spectra for the reaction between **DFC-EN-*p*-Ph-NO$_2$** and Al^{3+}. Each spectrum was taken at an interval of 50 seconds for initial 10 spectra and then it was recorded at an interval of 100 seconds. As the reaction between probe and Al^{3+} is relatively slow each spectrum for absorption titration was recorded after 2 hour of mixing.

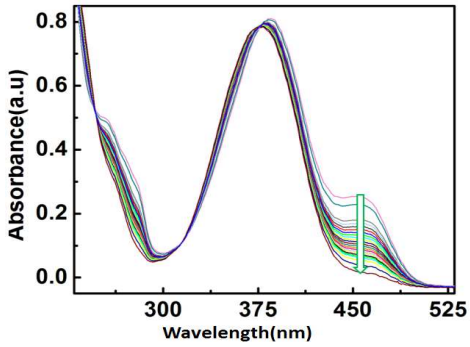

Fig. 3.Time resolved spectra for the reaction between the probe **DFC-EN-*p*-Ph-NO$_2$ and Al^{3+}** in MeOH-H_2O (8:2, v/v) at pH 7.2 (10 mM HEPES buffer), μ = 0.05 M (LiCl), temperature 25 ºC. First spectrum was taken immediately after mixing and subsequent spectra were taken at a time interval of 60 seconds.

Fluorescence studies

Due to excited state intramolecular proton transfer (**ESIPT**) from the phenolic –OH to azomethyn-N atom along with the C=N isomerization, the free ligand shows very weak fluorescence behaviour at 520 nm. But on complexation with Al^{3+} both these processes are effectively blocked and the probe becomes highly fluorescencent through chelation enhanced fluorescence (**CHEF**) effect resulting a large enhancement in the fluorescence intensity at 486 nm accompanied with 34 nm blue (**Fig. 4**). The mechanism is shown in **Scheme 1.** A proton transfer and C=N isomerization might also affect the "second" azomethin group in the molecule, even after chelation of one Al^{3+} ion.

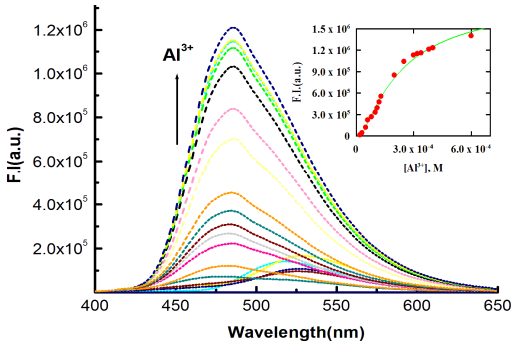

Fig. 4. (a) Fluorescence titration of 20 μM**DFC-EN-*p*-Ph-NO$_2$** in MeOH-H_2O (8:2, v/v) in HEPES buffer at pH 7.2 by the gradual addition Al^{3+} with λ_{ex}= 370 nm, λ_{em} = 486 nm Inset (b) non-linear curve-fit of F.I vs. [Al^{3+}].

The fluorescence titrations were carried out in three ways. (a) In the first step we kept ligand concentration fixed at 20 μM and [Al^{3+}] varied between 0 and 380 μM and Fluorescence intensity (FI) at

486 nm were recorded (λ_{ex} = 370 nm) at a fixed time interval of 30 min to allow the reaction to complete, as the reaction between the probe and Al^{3+} was found to be slower. When we plot FI as a function of [Al^{3+}] we get a non-linear curve of decreasing slope which was solved by fitting the titration data to eqn 1 and the corresponding evaluated parameters are: K_f = (5.29 ± 1.11) x 10^4 M^{-1} and n = 1.30 ± 0.02 which clearly signifies a 1:1 complexation between **DFC-EN-*p*-Ph-NO_2** and Al^{3+}.The detection limit as determined by 3σ method was found to be 7.55 μM (**Fig.S6**)

In a second attempt (b) we have treated 20 μM probe with 380 μM [Al^{3+}] and then added PPi gradually upto 230 μM which showed a gradual decay of FI with added PPi. First spectrum was taken within 10 sec of mixing and subsequently each spectrum was recorded at a time interval of 30 sec. This decrease in FI may be attributed to the displacement of Al^{3+} from Al^{3+}–PPi complex and this arises due to a stronger affinity of Al^{3+} towards PPi over the probe. On further addition of PPi to this mixture there was a gradual increase in FI at 534 nm which may be due to H-bonding interaction between the probe and PPi (**Fig.S7**) giving a rigid structure to the probe and blocking both the ESIPT and isomerization across the C=N (azomethyne) bond. Finally, (c) to confirm the proposition in (b) we have carried out this titration in the absence of Al^{3+} and indeed there is a gradual increase in FI at 534 nm on increasing the concentration of PPi. A plot of FI at vs. PPi gives non-linear curve and solved by fitting the titration data to eqn 1 and the evaluated parameters are: K_f = (1.34 ± 0.81) x 10^3 M^{-1} and n = 0.94 ± 0.07.(**Fig. 5**). In order to check the applicability of the probe at lower concentration we have carried out experiments keeping probe concentration at 2 μM and then treated with increasing concentration of Al^{3+} and PPi separately and we observed significant enhancement of FI at 484 and 534 nm respectively, suggesting its applicability at lower concentration (at least at 2 μM).

The selective sensing of analyte is an important criterion of a successful sensor. In order to check the selectivity of **DFC-EN-*p*-Ph-NO_2** towards Al^{3+} we have carried out steady state fluorescence experiments with 20 μM **DFC-EN-*p*-Ph-NO_2** and 5 equivalents of different metal ions both in absence and presence of Al^{3+}. It was interesting to note that the detection of Al^{3+} was not perturbed by biologically abundant metal ions like Na^+, K^+, Ca^{2+} etc and transition metal ions, namely Cr^{3+}, Mn^{2+}, Fe^{2+}, Fe^{3+}, Co^{2+}, Ni^{2+}, Cu^{2+}, as well as heavy metal ions like Cd^{2+}, Pb^{2+}, and Hg^{2+}(**Fig. 6**).

With the addition of PPi, there is an enhancement in fluorescence intensity (~5 fold) at 534 nm which is red shifted from 520 nm on excitation at 370 nm). The detection limit is found to be 3.34 μM (**Fig. S6a**) indicating a high sensitivity of the ligand towards PPi. No significant changes were observed in the emission spectra by the addition of the other anions such as HPO_4^{2-}, PO_4^{3-}, ATP, AcO^-, Cl^-, Br^-, F^-, SO_4^{2-}, SCN^- and N_3^-, AsO_4^-, $S_2O_4^-$, NO_2^- under similar experimental conditions. The selectivity for PPi with 20 μM of **DFC-EN-*p*-Ph-NO_2** was plotted as a bar diagram in **Fig.7.** Interestingly, anions other than PPi that contain the phosphate moiety do not interfere in the sensing of PPi, except ATP where a slight FI enhancement was noted.

The described sensor shows turn on fluorescent response to Al^{3+} and PPi so the two analytes may interfere with each other during the detection. To short out how to avoid the possible interference from each other we have carried out two experiments. In one case, to 20 μM probe, ~17 equivalents of Al^{3+} was added and then PPi was added incrementally. The emission band at 486 nm is abruptly quenched on addition of ~12 equivalents of PPi (**Fig. S7**) and a new peak at 534 nm is started to grow on further addition of PPi to the solution mixture and becomes constant at [PPi]= 700 μM **(Fig.S7)**.

In another experiment, to a 20 μM probe, 700 μM (35 equivalents) PPi was added and then Al^{3+} was added incrementally. It was observed that emission peak at 534 for DFC-en-*p*-Ph-NO_2—PPi complex starts to diminish with the increase in concentration of Al^{3+}, becomes almost the same as that of in pure probe at 950 μM of Al^{3+} and then a peak at 484 nm for DFC-en-*p*-Ph-NO_2—Al^{3+} complex stars to grow on further increasing the concentration of PPi and becomes constant at [Al^{3+}] = 1225 μM. These two experiments clearly demonstrate the reversibility and selectivity of the probe towards Al^{3+} and PPi; one being higher in concentration over the other **(Fig.S8).** The quantum yield value for free **DFC-EN-*p*-Ph-NO_2** and **DFC-EN-*p*-Ph-NO_2–Al^{3+}, DFC-EN-*p*-Ph-NO_2–PPi** ensembles are 0 .002, 0.011, 0.003 respectively.

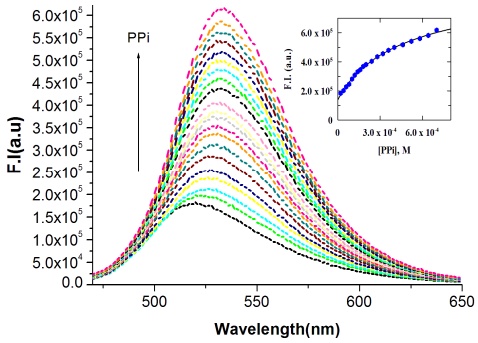

Fig. 5. (a) Fluorescence titration of 20 μM **DFC-EN-*p*-Ph-NO_2** in MeOH-H_2O (8:2, v/v) in HEPES buffer at pH 7.2 by the gradual addition PPi with λ_{ex} = 370 nm, λ_{em} = 534 nm Inset (b) non-linear curve-fit of F.I vs. [PPi] and the evaluated parameters are: K_f = (1.34 ± 0.81) x 10^3 M^{-1} and n = 0.94 ± 0.07.

The strong solvatochromic behavior was observed for the free ligand **(DFC-EN-*p*-Ph-NO_2),** as well as its complexes with Al^{3+} **(DFC-EN-*p*-Ph-NO_2-Al)** and PPi **(DFC-EN-*p*-Ph-NO_2-PPi)**. In all cases there are red shifts of absorption maximum on increasing the solvent polarity which clearly indicates that there is charge separation in the excited state and interact strongly with more polar solvents (**Fig. S9**). In case of fluorescence emission spectra we observed solvent polarity dependent blue shift for **DFC-EN-*p*-Ph-NO_2** and red shift for **DFC-EN-*p*-Ph-NO_2-Al** and **DFC-EN-*p*-Ph-NO_2-PPi**. The blue shift in λ_{em} of the free probe may be rationalized by considering low charge separation in the excited state compared to the ground state, possibly due to attainment of planar structure in the excited state. In other cases normal behaviour (red shift) is apparent (**Fig.8** and **Fig. S9).**This is confirmed by a plot of Plot of Stokes shift ($\overline{\Delta\nu}$) vs solvent polarity parameter $E_T(30)$ in different solvents (Fig. S15-S17).[29]

Journal Name RSCPublishing

ARTICLE

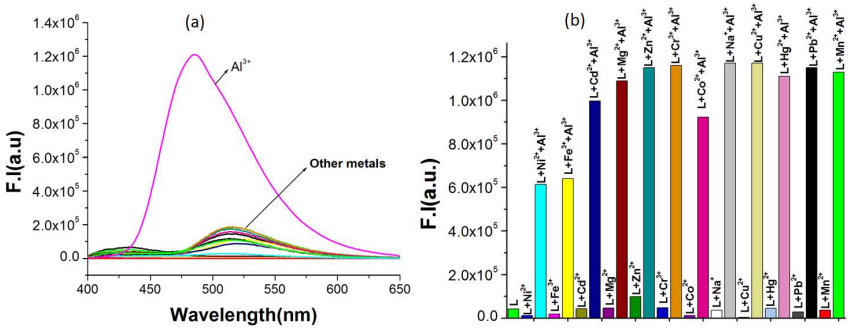

Fig. 6. (a) Fluorescence response of different metal ions towards **DFC-EN-*p*-Ph-NO$_2$**(20 μM); (b) Interference from other metal cations in a binary mixture: **L(DFC-EN-*p*-Ph-NO$_2$)** (20 μM) + Al^{3+} (380 μM) + M^{n+} (5 equivalent than Al^{3+}), where M^{n+} = Ni^{2+}, Fe^{3+}, Cd^{2+}, Mg^{2+} , Zn^{2+}, Cr^{3+}, Co^{2+}, Na^{+}, Cu^{2+}, Mn^{2+}, Hg^{2+}, Pb^{2+} and Mn^{2+} . **Mix** = (Ni^{2+}, Fe^{3+}, Cd^{2+}, Mg^{2+} , Zn^{2+}, Cr^{3+}, Co^{2+}, Na^{+}, Cu^{2+}, Mn^{2+}, Hg^{2+}, Pb^{2+}, Mn^{2+}) were present together with **L** and Al^{3+} (in MeOH-H_2O (8:2, v/v) in HEPES buffer at pH 7.2 , λ_{ex}= 370 nm, λ_{em} = 486 nm). Each spectra was drawn after 15 mins.

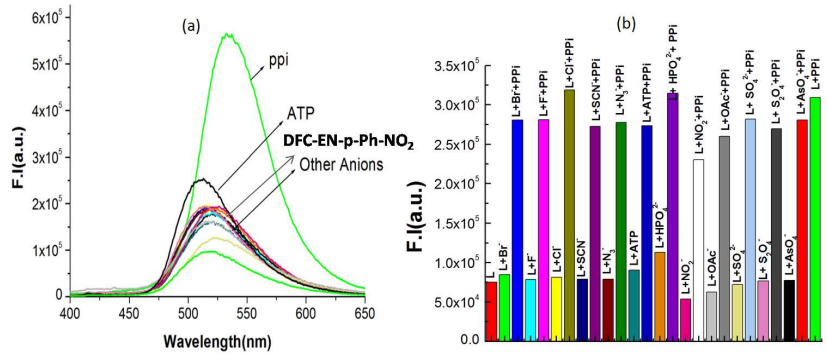

Fig. 7.(a) Fluorescence response of different anions towards **DFC-EN-*p*-Ph-NO$_2$** (20 μM); (b) Interference from other anions in a binary mixture: **L(DFC-EN-*p*-Ph-NO$_2$)** (10 μM) + PPi (350 μM) + X^{n-} (5 equivalent than PPi), where X^{n-} = Br^-, F^-, Cl^-, SCN^- , N_3^-, ATP , HPO_4^{2-}, NO_2^-, OAc^-, SO_4^{2-}, $S_2O_4^-$, AsO_4- and PPi . **Mix** = (Br^-, F^-, Cl^-, SCN^- , N_3^-, ATP , HPO_4^{2-}, NO_2^-, OAc^-, SO_4^{2-}, $S_2O_4^-$, AsO_4-) were present together with **L** and PPi (in MeOH-H_2O (8:2, v/v) in HEPES buffer at pH 7.2 , λ_{ex}= 370 nm, λ_{em} = 534 nm).

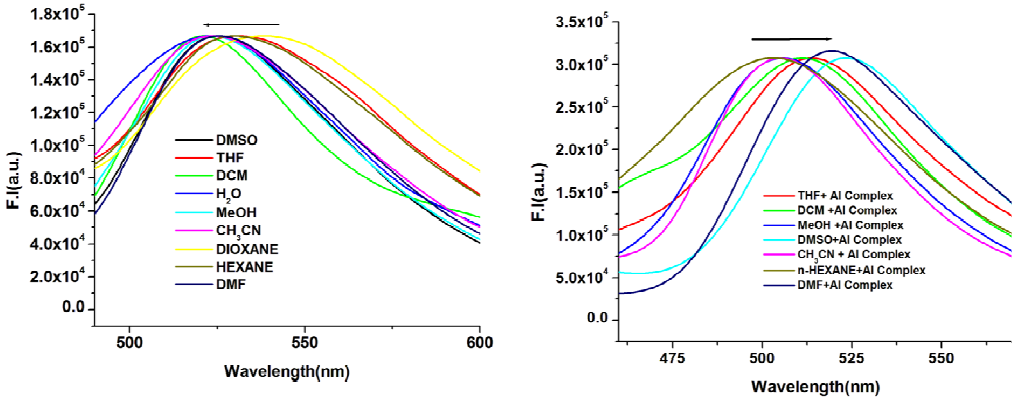

Fig.8. Polarity dependent blue shift of λ_{em} of the ligand (non-polar to polar) and red shift of λ_{em} of the Al-complex (non-polar to polar)

Journal Name

RSCPublishing

ARTICLE

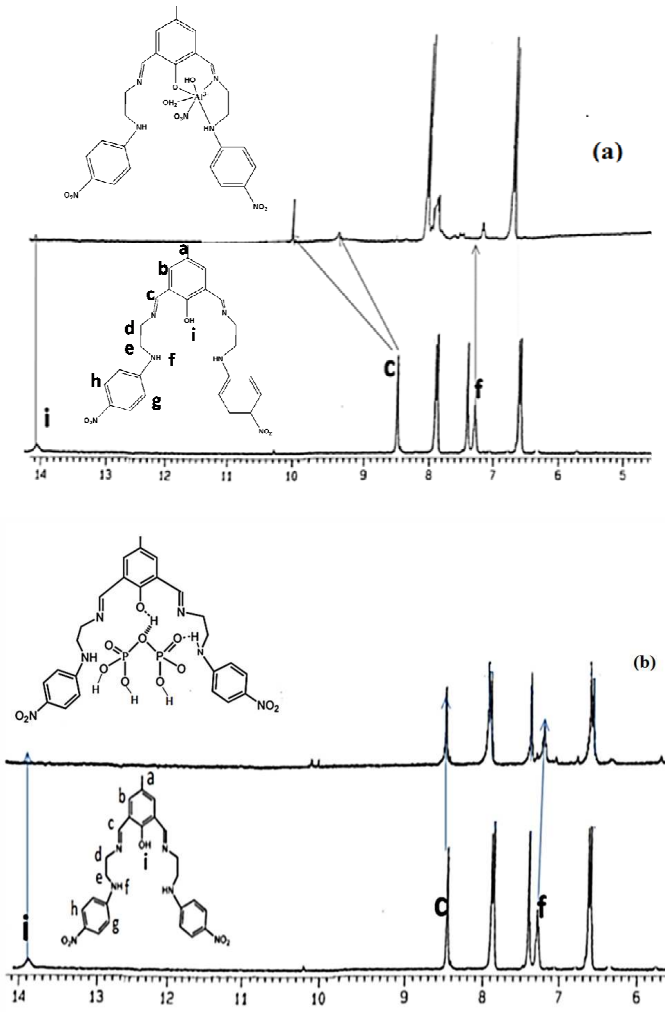

Fig. 9. (a) ^{1}H-NMR shifts of free ligand and with addition of 1.5 equivalents of and Al^{3+} (b) PPi in DMSO-d_6 recorded on a 300 MHz Bruker 50 NMR spectrometer.

The coordination mode of **DFC-EN-*p*-Ph-NO$_2$** towards Al^{3+} was supported by ^{1}H-NMR studies (**Fig. 9**) which clearly showed a down field shift of azomethine protons (c) in **DFC-EN-*p*-Ph-NO$_2$ –**Al^{3+} complex from 8.57 of the free ligand to 9.42, 10.17 in the complex. **[Fig. 9(a)]** The larger shift and splitting into two peaks are due to strong binding of one azomethine N to Al^{3+} while other decoupled from H-bonding with phenolic –OH proton (**Table S1**). In the free ligand there is intramolecular H-bonding between azomethyne-N and –OH proton (i) resulting a downfield shift of -OH proton signal to 14.04 ppm and appears as a broad signal, which vanishes completely on complexation with Al^{3+}. The up-field shift of imine-NH proton (f) signal from 7.36 to 7.17 in complex **[Fig. 9(a)]** is due to electronic environment. In case of DFC-**EN-*p*-Ph-NO$_2$**–PPi complex this OH proton signal is broadened and almost vanishes. The azomethine proton (c) remains almost unchanged (7.36 to 7.25) or slightly up-field shifted due to non-participation in H-bonding to PPi and shift of imine–NH proton (f) towards up-field occurs due to H-bonding **[Fig. 9(b)]**.

We have also carried out DFT calculations on **DFC-EN-*p*-Ph-NO$_2$**, **DFC-EN-*p*-Ph-NO$_2$** – Al^{3+} and **DFC-EN-*p*-Ph-NO$_2$** – PPi to strengthen the coordination modes of the ligand towards Al^{3+} and PPi and their optimized geometries are shown in **Fig S10**. The TDDFT calculations on free ligand and its Al^{3+} complex were used to generate their UV-Vis spectra which showed excellent match in λ_{max} with experimental findings (**Table S4).** A blue shift in the absorption spectrum of **DFC-EN-p-Ph-NO$_2$**–Al^{3+} complex compared to free ligand is also rationalized by comparing the HOMO–LUMO+1 gap for these species which is slightly higher for the former (ΔE =3.46eV , λ_{theo}=370) than the later (ΔE=3.27eV, λ_{theo}=388) (**Fig 10**).

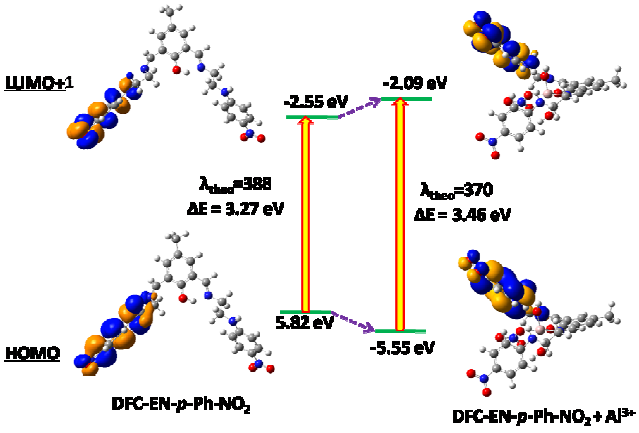

Fig.10. Comparable pictogram of blue shift transition in electronic spectra in form of energy difference.

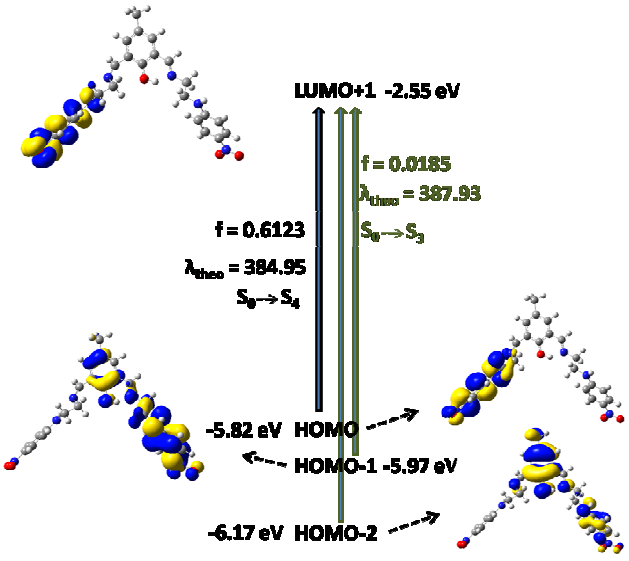

Fig.11. Frontier molecular orbitals involved in the UV-Vis absorption of **DFC-EN-*p*-Ph-NO$_2$.**

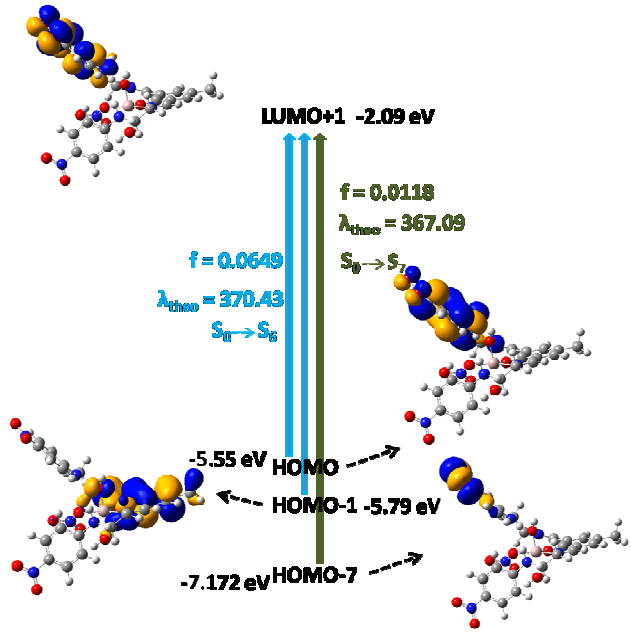

Fig.12. Frontier molecular orbitals involved in the UV-Vis absorption of **DFC-EN-*p*-Ph-NO$_2$+Al^{3+}**

Cell imaging experiments

The obvious excellent sensing capability of **DFC-EN-*p*-Ph-NO$_2$** towards PPi and Al^{3+} were further scrutinized in HCT116 cell lines. The cytotoxic effect of DFC-**EN-*p*-Ph-NO$_2$** towards HCT116 cells was determined by MTT assay which showed no severe cytotoxicity till 60 μM (<30% cytotoxicity) of **DFC-EN-*p*-Ph-NO$_2$** and more than 89.11% cell viability was observed at 10 μM (**Viability curve** (**Fig. S12**)). Hence further experiments were carried out with safer 10 μM of **DFC-EN-*p*-Ph-NO$_2$**. When **DFC-EN-*p*-Ph-NO$_2$** (10 μM) was treated with HCT116 cells for 30 min at 37°C, it did not show intracellular fluorescence (**Fig. 13**). The gradual increase in the blue (for Al^{3+}) and green (for PPi) fluorescence was observed with increase in concentration of Al^{3+} and PPi, respectively. When **DFC-EN-*p*-Ph-NO$_2$** (10 μM) form 1:1 intra cellular complex with Al^{3+} (10 μM, 30 min at 37°C) it gives intense blue fluorescence. However, when **DFC-EN-*p*-Ph-NO$_2$** (10 μM) was treated with PPi (10 μM, 30 min at 37°C) green fluorescence was observed intracellularly, but no blue fluorescence suggesting that **DFC-EN-*p*-Ph-NO$_2$** +PPi complex shifts emission wavelengths to green region (red shift). In another experiment **DFC-EN-*p*-Ph-NO$_2$** –Al^{3+} ensemble (10 μM each) when treated with 10 μM PPi the blue fluorescence of **DFC-EN-*p*-Ph-NO$_2$** –Al^{3+} complex is almost vanishes, but in presence of large excess of PPi green fluorescence corresponding to **DFC-EN-*p*-Ph-NO$_2$** –PPi ensemble becomes visible. This suggests that **DFC-EN-*p*-Ph-NO$_2$** could form optimum stable fluorescence complex when incubated with either PPi or Al^{3+} ions separately. The dual fluorescence sensory behaviour of **DFC-EN-*p*-Ph-NO$_2$** towards Al^{3+} and PPi was dependent on the ion to which it binds thereby opening up its vast application towards biological sensing of these ions with good photo stability and very low cytotoxicity at low concentration region (10 μM). Thus **DFC-EN-*p*-Ph-NO$_2$** facilitates the selective sensing of either PPi or Al^{3+} and serves as the biomonitoring and cell imaging tool for PPi and Al^{3+}.

Finally, to understand the selective interaction of **DFC-EN-*p*-Ph-NO$_2$** with PPi over ATP and Pi DFT calculations were performed to attain the optimized geometry of **DFC-EN-*p*-Ph-NO$_2$** and its complexes with PPi, ATP and Pi (2) **(Fig. S11**). From this study, it is clear that the energy gap between the highest occupied molecular orbital (HOMO) and the lowest unoccupied molecular orbital (LUMO) are 3.08. 3.48. 2.84 and 1.66 eV for free ligand and its complexes with Pi, ATP, and PPi, respectively. It is to be noted that **DFC-EN-*p*-Ph-NO$_2$**–PPi has the lowest energy gap giving rise to a more stable species,[30] while **DFC-EN-*p*-Ph-NO$_2$**–ATP has next lower energy gap and this is reflected by substantial change in FI in case of former and very low FI change in case of later. In case of **DFC-EN-*p*-Ph-NO$_2$**–Pi no observable change in FI was observed.

.

Conclusion

In summary, we have successfully developed a new dual channel chemical sensor for the detection of Al^{3+} and pyrophosphate ions (PPi) together or separately. The probe **DFC-EN-*p*-Ph-NO$_2$** or **DFC-EN-*p*-Ph-NO$_2$**–Al^{3+} ensemble showed a highly sensitive and selective response to PPi in presence of other anions like HPO_4^{2-}, PO_4^{3-}, ATP, AcO^-, Cl^-, Br^-, F^-, SO_4^{2-}, SCN^- and N_3^-, AsO_4^-, $S_2O_4^-$ and NO_2^- at pH 7.4 by fluorescent change in organo-aqueous solutions. In particular, the fluorescent detection of PPi was not interfered by the presence of 400 μM of ATP or Pi. Overall results

indicate that the dual signal chemosensing of PPi by **DFC-EN-*p*-Ph-NO_2** or **DFC-EN-*p*-Ph-NO_2** –Al^{3+} ensemble may contribute to the development of more efficient and useful methods for detecting PPi in biological systems. Its solubility in bio-compatible solvent (DMSO/H_2O 1:99 v/v) and cell permeability with no or negligible cytotoxicity provide good opportunity towards *in-vitro*/*in-vivo* cell imaging studies of these ions. The obvious excellent sensing capability of **DFC-EN-*p*-Ph-NO_2** towards PPi and Al^{3+} were further scrutinized in HCT116 cell lines. The modes of binding between **DFC-EN-*p*-Ph-NO_2** with Al^{3+} and PPi were established by DFT calculations.

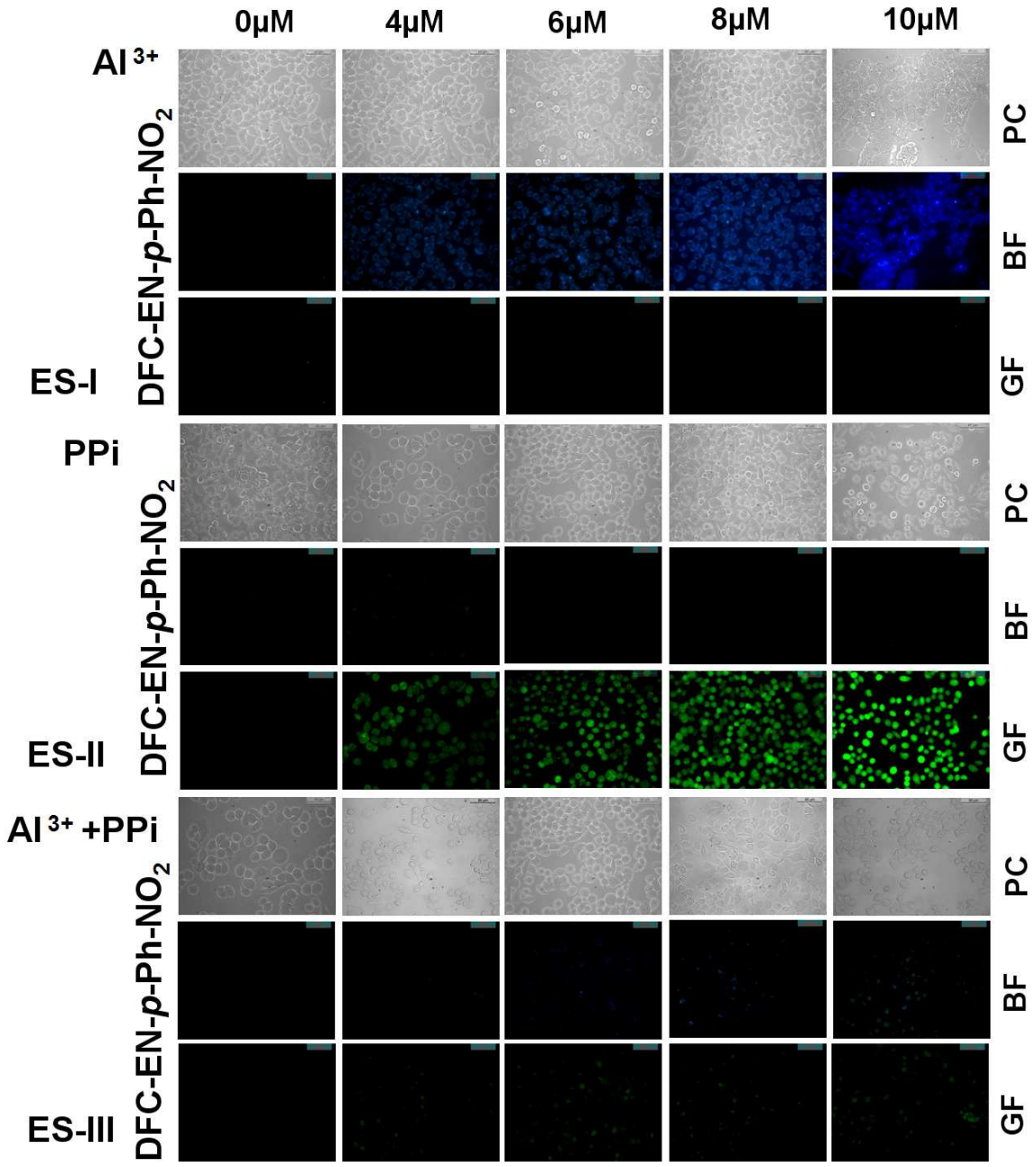

Fig. 13: The phase contrast and fluorescence images of HCT116 cells captured (40X) after cells were preincubated with **DFC-EN-*p*-Ph-NO_2 for** 30min at 37ºC in the incubator followed by washing with 1XPBS for 3 time and allowed to treated with 0μM, 4μM, 6μM, 8μM and 10μM Al^{3+} (ES-I), PPi (ES-II) and Al^{3+}+PPi (ES-III) for 30 min at 37°C. The image shows the strong blue florescence when **DFC-EN-*p*-Ph-NO_2** complexes with Al^{3+} and green fluorescence with PPi in blue and green filter respectively. The gradual increase in the blue (for Al^{3+}) and green (for PPi) fluorescence was observed with increase in concentration of Al^{3+} and PPi. ES; Experimental Set, PC; Phase Contrast, BF; Blue filter, GF; Green filter. Cell imaging studies were carried out three times.

Journal Name RSCPublishing

ARTICLE

Acknowledgement. Financial supports from CSIR (Ref. 02(2490)/11/EMR-II) and DST (Ref. SR/S1/IC-20/2012) New Delhi are gratefully acknowledged.

Supporting Information Available. Electronic Supplementary Information (ESI) available: experimental details regarding the synthesis and characterization of the ligand including spectroscopic details. For ESI format see DOI: 10.1039/c000000x/

Authors' Address

[a] Department of Chemistry, Jadavpur University, Kolkata 700 032, India, Fax: 91-33-2414-6223, E-mail: m_ali2062@yahoo.com

[b] Molecular & Human Genetics Division, CSIR-Indian Institute of Chemical Biology, 4 Raja S.C. Mallick Road, Kolkata-700032, India

References

1 C. P. Mathews, K. E. van Hold, *Biochemistry*, The Benjamin/ Cummings Publishing Co., Inc., Redwood City, CA, 1990.

2 M. Ronaghi, S. Karamohamed, B. Pettersson, M. Uhlen and P. Nyren, *Anal. Biochem*.,1996, **242,** 84.

3 S. Xu, M. He, H. Yu, X. Cai, X. Tan, B. Lu and B. Shu, *Anal. Biochem*., 2001, **299**, 188.

4 K.D. Lopacinska and J. B. Strosznajder, *J. Physiol. Pharmacol*., 2005, **56**, 15.

5 M. Kamenetsky, S. Middelhaufe, E. M. Bank, L. R. Levin, J. Buck and C. Steegborn, *J. Mol. Biol*.2006, **362**, 623.

6 (*a*) M. T. Averbuch-Pouchot and A. Durif, World Scientific Publishing Co. Ptv. Ltd., Singapore, 1996;(*b*) R. A. Molins, CRC Press. Inc., Boca Raton,1991.

7 D. H. Vance and A. W. Czarnik, *J. Am. Chem. Soc*.,1994, **116**, 9397.

8 X. Zhao, Y. Liu and K. S. Schanze, *Chem. Commun*., 2007, 2914.

9 D. Aldakov and P. Anzenbacher Jr, *J. Am. Chem. Soc*., 2004, **126**,4752.

10 S. K. Kim, D. H. Lee, J. I. Hong andJ.Yoon, *Acc. Chem. Res*.2009,**42**, 23.

11 D. H. Lee, J. H. Im, S. U. Son, Y. K. Chung, J. I. Hong, *J. Am. Chem. Soc*., 2003**, 125**, 7752.

12 C. Park and J.-I. Hong, *Tetrahedron Lett.*, 2010, **51**, 1960.

13 S. Watchasit, A. Kaowliew, C. Suksai, T. Tuntulani, W. Ngeontae and C. Pakawatchai, *Tetrahedron Lett.*,2010, **51**, 3398.

14 S. Mizukami, T. Nagano, Y. Urano, A. Odani and K. Kikuchi, *J. Am. Chem. Soc*., 2002, **124**, 3920.

15 K. M. K. Swamy, S. K. Kwon, H. N. Lee, S. M. S. Kumar, J. S. Kim and J. Yoon, *Tetrahedron Lett.*, 2007, **48**, 8683.

16 N. Shao, J. Jin, G. Wang, Y. Zhang, R. Yang and J. Yuan, *Chem. Commun.*, 2008, 1127.

17 C. M. G. dos Santos and T. Gunnlaugsson, *Dalton Trans.,* 2009, **24**, 4712.

18 C. R. Loran, J.-M. Kim, S. -Y. Chung, J. Yoon and K.-H. Lee, *Analyst*, 2010, **135**, 2079.

19 S. K. Kim, D. H. Lee, J.-I. Hong and J. Yoon, *Acc. Chem. Res*., 2009, **42**, 23.

20 S. Mizukami, T. Nagano, Y. Urano, A. Odani and K. Kikuchi, *J. Am. Chem. Soc*., 2002, **124**, 3920.

21 H. N. Lee, K. M. K. Swamy, S. K. Kim, J. Y. Kwon, Y. Kim, S.J. Kim, Y. J. Yoon and J. Yoon, *Org. Lett*., 2007, **9**, 243.

22 H. N. Lee, Z. Xu, S. K. Kim, K. M. K. Swamy, Y. Kim, S. J. Kim and J. Yoon, *J. Am. Chem. Soc*., 2007, **129**, 3828.

23 H. K. Cho, D. H. Lee and J. I. Hong, *Chem. Commun*., 2005,1690.

24. J. Wang, Y. Xiao, Z. Zhang, X. Qian, Y. Yang and Q. Xu, *J. Mater. Chem.,* 2005, **15**, 2836.

25 R. Alam, T. Mistri, A.Katarkar, K. Chaudhuri, S. K. Mandal, A. R. Khuda-Bukhsh K. K. Das and M. Ali**,** *Analyst,* 2014, **139**, 4022**.**

26 J. Ratha, K. A. Majumdar, S. K. Mandal, R. Bera, C. Sarkar, B. Saha, C. Mandal, K. D. Saha and R. Bhadra, *Mol. Cell. Biochem*., 2006, **290**, 113.

27 S. Chall, S. S. Mati, S. Konar, D. Singharoy and S.C. Bhattacharya, *Org. Biomol. Chem.,* 2014, **12**, 6447.

28 R. Alam, T. Mistri, P. Mondal, D. Das, S. K. Mandal, A.R. Khuda-Bukhsh and M. Ali, *Dalton Trans*., 2014, **43,** 2566.

29 S. S. Mati, S. Sarkar, S. Rakshit,A. Sarkar and S.C. Bhattacharya, RSC Adv., 2013, **3**, 8071

30 S. Lohar, S. Pal, B. Sen, M. Mukherjee, S. Banerjee, and P. Chattopadhyay, *Anal. Chem*. 2014, **86**, 11357.